Quasi-Static Analysis of Shielded Microstrip Transmission Lines with Thick Electrodes

N. H. Zhu, W. Qiu, E. Y. B. Pun, and P. S. Chung

***Abstract*— An extended point-matching method for analyzing the shielded microstrip transmission lines with thick electrodes has been developed based on [1]. This method provides a simple and fast approach to the quasi-static analysis of the structures. The calculated fields are used to estimate the characteristic impedance and effective dielectric constant of the structures. The results agree well with available theoretical results obtained using other methods, such as the finite element method and the boundary element method. This method can be further applied to other microstrip lines widely used in monolithic microwave integrated circuits (MMIC's) applications.**

***Index Terms*—Point-matching method, shielded microstrip lines.**

I. Introduction

With the growing interest in microstrip transmission lines for monolithic microwave integrated circuits (MMIC's) applications, the need for an accurate and fast modeling of the structures has increased. It has been shown that the metallization thickness plays a very important role in the propagation characteristics and the electric field distributions in the structures. Quasi-static solutions to the structures with finitely thick electrodes have been obtained using various methods, such as a mixed spectral-space domain method [2], the analysis based on the mode-matching method [3], [4], the conformal mapping techniques [5], the finite difference method [6], the finite element method [7]–[9], the boundary element method [10], [11], the step current density approximation [12], and the method of lines [13].

The point-matching method has been used to calculate the electrical potential and the fields generated by a set of electrodes placed on top of a layered dielectric medium [1]. However, the analysis is carried out under the assumption of infinitely thin electrodes. The point-matching method has been used to analyze the shielded microstrip lines with finite-strip metallization thickness [14]. The disadvantage of this method is that there is a strong correlation between the number of boundary points considered and the rank of the system matrix. This method can lead to acceptable results only when the strip-width-to-thickness ratio *W/T* is larger than 100 [14]. In this paper, the point-matching method [1] is extended to analyze shielded microstrip transmission lines with thick electrodes. Typically, the value of the electrode-width-to-thickness ratio is below ten. Comparison is made between our calculated results and available theoretical results obtained using other methods.

II. Formulation

The single and coupled shielded microstrip lines fabricated on a two-layered dielectric substrate, considered in [2], are shown in Fig. 1. In the analysis, the structures are divided into five regions, with both the shielding box and strips assumed to be perfectly conducting. For the structure shown in Fig. 1(a), the potential functions in terms of the Fourier-sine series satisfying the Laplace equation and part of boundary conditions can be expressed as

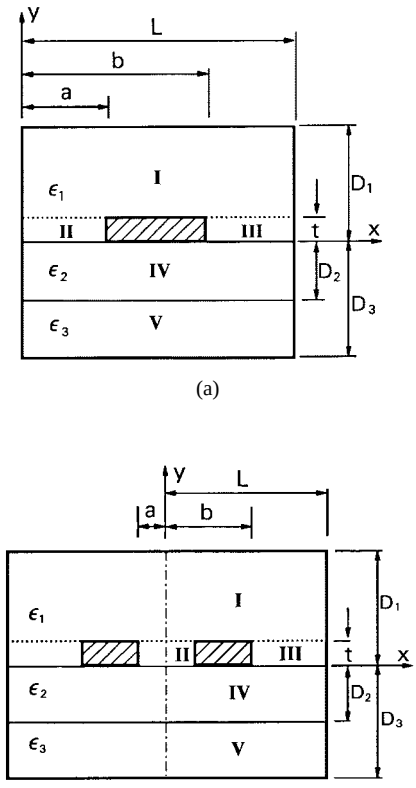

Fig. 1. (a) Single and (b) coupled shielded microstrip lines with finitely thick electrodes on a two-layered dielectric substrate.

$$\phi_1 = \sum_{i=1}^{N_1} a_i \sinh\left(\frac{i\pi(y-D_1)}{L}\right)\sin\left(\frac{i\pi x}{L}\right) \tag{1a}$$

$$\phi_2 = \frac{\phi_0 x}{a} + \sum_{j=1}^{N_2}\left[b_j \exp\left(-\frac{j\pi y}{a}\right) + c_j \exp\left(\frac{j\pi y}{a}\right)\right]\sin\left(\frac{j\pi x}{a}\right) \tag{1b}$$

$$\phi_3 = \frac{\phi_0(L-x)}{L-b} + \sum_{k=1}^{N_3}\left[d_k \exp\left(-\frac{k\pi y}{L-b}\right) + e_k \exp\left(\frac{k\pi y}{L-b}\right)\right]\sin\left(\frac{k\pi(x-b)}{L-b}\right) \tag{1c}$$

$$\phi_4 = \sum_{i=1}^{N-1}\left[f_i \exp\left(-\frac{i\pi y}{L}\right) + g_i \exp\left(\frac{i\pi y}{L}\right)\right]\sin\left(\frac{i\pi x}{L}\right) \tag{1d}$$

$$\phi_5 = \sum_{i=1}^{N_1} h_i \sinh\left[\frac{i\pi(y+D_3)}{L}\right]\sin\left(\frac{i\pi}{L}x\right) \tag{1e}$$

where ϕ_0 is the potential applied to the strip, a_i, b_j, c_j, d_k, e_k, f_i, g_i, and h_i are coefficients to be determined. The series are truncated with different numbers N_1, N_2, and N_3. The matching points do not include the points $x = 0$ and $x = L$, i.e., $x_i = i\Delta x = iL/N, i = 1, 2, \cdots, N-1$. N_1, N_2, and N_3 are set to be $N-1$, $(a/L)N$, and

Manuscript received July 26, 1995; revised October 18, 1996. This work was supported in part by the Science Foundation of Guangdong Province, R.O.C., the Croucher Foundation, and a Strategic Grant from City University of Hong Kong, Kowloon, Hong Kong.

N. H. Zhu is with the Electronics Department, Zhongshan University, Guangdong 510275, R.O.C.

W. Qiu, E. Y. B. Pun, and P. S. Chung are with the Department of Electronic Engineering, City University of Hong Kong, Kowloon, Hong Kong.

Publisher Item Identifier S 0018-9480(97)00838-7.

$(L-b)N/L$, respectively. By employing the boundary conditions in the plane $y=-D_2$, f_i and g_i depend unambiguously on h_i [1]. a_i, b_j, c_j, d_k, e_k, and h_i are assumed to be independent variables, and the exact relations among them are not required since the derivations of these relations are very complicated [4]. In the planes $y=0$ and $y=t$, the continuities of both E_x and $\varepsilon_y E_y$ are satisfied, while on the strip the potential functions are required to be equal to the applied V. This leads to $M=2N-2+2aN/L+2(L-b)N/L$ equations which can be converted into a matrix equation. The unknown coefficients can be easily determined by solving this matrix equation. There is no need for evaluating integrals and iterations. The effective dielectric constant and characteristic impedance of the structure can be determined by calculating the electric charges in the strip [15].

For the coupled shielded microstrip line shown in Fig. 1(b), both c- and π-modes can be resolved into even and odd modes [15]. Therefore, only the even and odd modes are discussed. For the odd mode, the plane $x=0$ is an electric wall, and the solutions have been given by (1). For the even mode, the plane $x=0$ is a magnetic wall and the matching points at $x=0$ are included. Thus the potential functions can be written as

$$\phi_1=\sum_{i=1}^{N_1} a_i \sinh\left(\frac{(2i-1)\pi(y-D_1)}{2L}\right)\cos\left(\frac{(2i-1)\pi x}{2L}\right) \tag{2a}$$

$$\phi_2=\phi_0+\sum_{j=1}^{N_2}\left[b_j\exp\left(-\frac{(2j-1)\pi y}{2a}\right)+c_j\exp\left(\frac{(2j-1)\pi y}{2a}\right)\right]\cos\left(\frac{(2j-1)\pi x}{2a}\right) \tag{2b}$$

$$\phi_3=\frac{\phi_0(L-x)}{L-b}+\sum_{k=1}^{N_3}\left[d_k\exp\left(-\frac{(2k-1)\pi y}{2(L-b)}\right)+e_k\exp\left(\frac{(2k-1)\pi y}{2(L-b)}\right)\right]\sin\left(\frac{(2k-1)\pi(x-b)}{2(L-b)}\right) \tag{2c}$$

$$\phi_4=\sum_{i=1}^{N_1}\left[f_i\exp\left(-\frac{(2i-1)\pi y}{2L}\right)+g_i\exp\left(\frac{(2i-1)\pi y}{2L}\right)\right]\cos\left(\frac{(2i-1)\pi x}{2L}\right) \tag{2d}$$

$$\phi_5=\sum_{i=1}^{N_1} h_i\sinh\left[\frac{(2i-1)\pi(y+D_3)}{2L}\right]\cos\left(\frac{(2i-1)\pi x}{2L}\right). \tag{2e}$$

For microstrip lines on a multilayered (more than two) substrate, the relations among the coefficients in the expansion series for the potentials in the substrate can be obtained by applying the boundary conditions. All these coefficients unambiguously depend on the coefficients of the potential expansion series in the bottom substrate layer and the order of the matrix equation will not increase. The representations of the potential functions for different structures have been discussed in detail in [1]. This extended point-matching method can also be applied to other coplanar lines on the multilayered substrate (i.e., coplanar waveguides, asymmetric coplanar lines, and structures without shielding planes), but different functional forms of the series expansions should be used.

III. Results and Discussions

We first calculate the effective dielectric constant and the characteristic impedance of a shielded microstrip line, with dimensions $a=1$ mm, $b=2$ mm, $L=5$ mm, $D_1=2$ mm, $D_2=1$ mm, $D_3=2$ mm, $\varepsilon_1=\varepsilon_3=\varepsilon_0$, and $\varepsilon_2=4\varepsilon_0$. The calculated results as a function of different truncation number N are shown in Fig. 2, where the parameter is the electrode thickness. It can be seen that the convergence is reasonably good even for a very thick electrode strip, thus confirming the practicality of our method. Our results are compared with those of the step-current density approximation [12], the boundary-element method [11], the finite-element method [8], and the technique proposed by [2]. Table I lists the calculated characteristic impedances of the shielded microstrip line with different combinations of thickness and width. Table II gives the calculated elements of the capacitance matrix for the coupled shielded coplanar strips considered in [2]. Close agreement with the published results has been obtained.

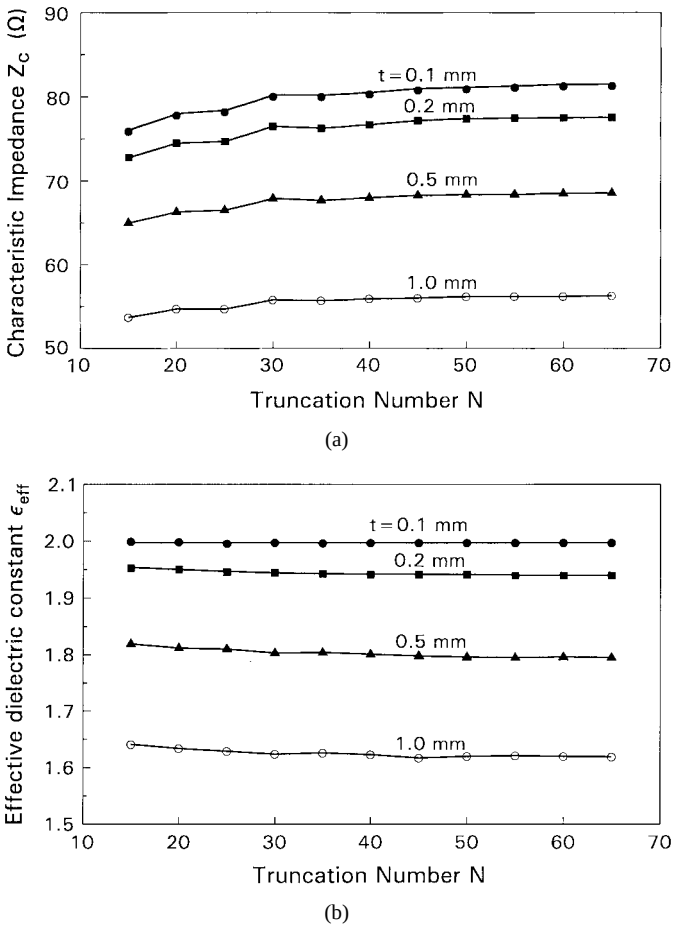

Fig. 2. Dependence of (a) the characteristic impedance and (b) the effective dielectric constant of the shielded microstrip line on the truncation number N. The parameter used is the electrode thickness t.

TABLE I
Calculated Characteristic Impedances for the Symmetric Single Planar Line Considered in [11]

t (mm)	W (mm)	Z_c (Ω) [12]	Z_c (Ω) [11]	Z_c (Ω) Our method
0.05	0.2	121.63	121.14	120.34
0.1	0.2	108.53	108.96	108.07
0.1	0.4	80.32	80.92	79.18
0.2	0.2	91.20	92.44	91.04
0.2	0.4	67.20	67.62	66.84
0.2	0.6	50.02	50.54	49.42

L=1mm, a=(L-W)/2, b=a+W, D_1+D_2=1mm, $D_2=D_1$-t, $D_3=D_2$, $\varepsilon_1=\varepsilon_2=\varepsilon_3=\varepsilon_0$

For the shielded microstrip line with dimensions: $L=10$ mm, $a=(L-W)/2$, $b=a+W$, $D_1=2$ mm, $D_2=1$ mm, $D_3=2$

TABLE II
CALCULATED ELEMENTS OF CAPACITANCE MATRIX FOR THE STRUCTURE CONSIDERED IN [8]

C_{11}=C_{22} (pF/m)	C_{12}=C_{21} (pF/m)	Ref.
108.1	-4.571	[2]
109.1	-4.712	[8]
108.8	-4.683	Our method

L=11mm, a=1mm, b=4mm, t=1mm, D_1=2.7mm, D_2=D_3=1mm, ε_1=ε_0, ε_2=ε_3=$2\varepsilon_0$

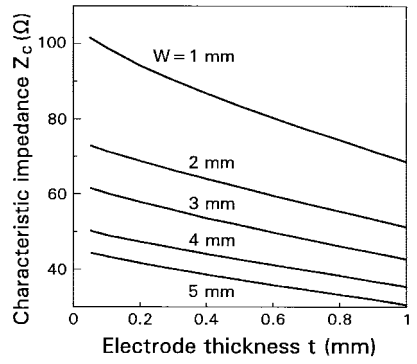

(a)

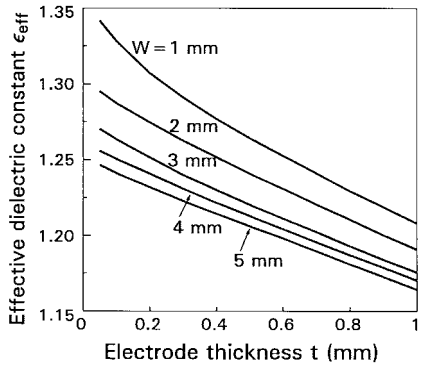

(b)

Fig. 3. (a) Characteristic impedance and (b) effective dielectric constant of the shielded microstrip line as a function of electrode thickness.

mm, $\varepsilon_1 = \varepsilon_3 = \varepsilon_0$, and $\varepsilon_2 = 4\varepsilon_0$, the characteristic impedance and effective dielectric constant are shown in Fig. 3 as a function of the electrode thickness, where the parameter is the electrode width $W = b - a$. The matching point are equidistantly spaced with a step of $\Delta x = L/N = 0.2$ mm. For the coupled shielded strips with dimensions: $W = b - a = 1$ mm, $L = 5$ mm, $D_1 = 2$ mm, $D_2 = 1$ mm, $D_3 = 2$ mm, $\varepsilon_1 = \varepsilon_3 = \varepsilon_0$, and $\varepsilon_2 = 4\varepsilon_0$, the characteristic impedance and effective dielectric constant of the even and odd modes are shown in Fig. 4 as a function of electrode thickness, where the parameter is $S = 2a$. The results given in [2, Fig. (6)] are also included in the figure. An excellent agreement between our results and the published data is obtained. It can be seen from Figs. 2–4 that our method can be used for the analysis of the microstrip transmission lines with thick electrodes.

IV. CONCLUSION

An extended point-matching method has been developed for the analysis of shielded microstrip lines with a small value of electrode-width-to-thickness ratio between one and ten. Compared to other

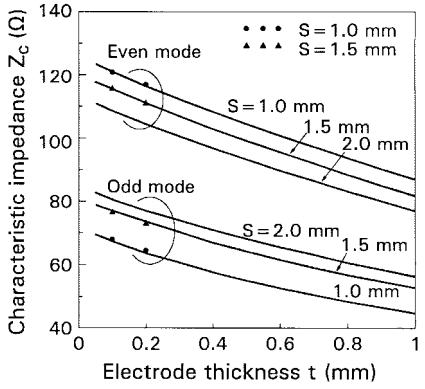

(a)

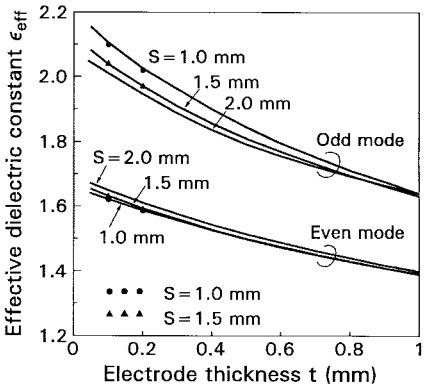

(b)

Fig. 4. (a) Characteristic impedance and (b) effective dielectric constant of the coupled shielded microstrips as a function of electrode thickness. The data given in [2, Fig. (6)] are also included.

methods [4], [2], and [16], the formulation of this method is very simple and there is no need for evaluating integrals and iterations. Our method is a faster, simpler, and more flexible technique, and can be further applied to analyze other structures, such as symmetric microstrip waveguides, asymmetric microstrip waveguide and strips, electrode structure without shielding planes, and structures with multilayered (more than two) dielectric substrate.

REFERENCES

[1] D. Marcuse, "Electrostatic field of coplanar lines computed with the point-matching method," *IEEE J. Quantum Electron.*, vol. 25, pp. 939–947, 1989.
[2] G. G. Gentili and G. Macchiarella, "Quasi-static analysis of shielded planar transmission lines with finite metallization thickness by a mixed spectral-space domain method," *IEEE Trans. Microwave Theory Tech..*, vol. 42, pp. 249–255, 1994.
[3] H. Vahldieck, M. Bèlanger, and Z. Jacubczyk, "A mode projecting method for the quasi-static analysis of electro-optic device electrodes considering finite metallization thickness and anisotropic substrate," *IEEE J. Quantum Electron.*, vol. 27, pp. 2306–2314, 1991.
[4] H. Jin, M. Bèlanger, and Z. Jacubczyk, "General analysis of electrodes in integrated-optics electro-optic devices," *IEEE J. Quantum Electron*, vol. 27, pp. 243–251, 1991.
[5] W. Heinrich, "Quasi-TEM description of MMIC coplanar lines including conductor-loss effects," *IEEE Trans. Microwave Theory Tech.*, vol. 41, pp. 45–52, 1993.
[6] H. E. Green, "The numerical solution of some important transmission line problems," *IEEE Trans. Microwave Theory Tech.*, vol. MTT-13, p. 676, 1965.
[7] Z. Pantic and R. Mittra, "Quasi-TEM analysis of microwave transmission lines by the finite-element method," *IEEE Trans. Microwave Theory Tech.*, vol. MTT-34, pp. 1096–1103, 1986.

[8] A. Khebir, A. Kouki, and R. Mittra, "High order asymptotic boundary condition for the finite element modeling of two-dimensional transmission line structures," *IEEE Trans. Microwave Theory Tech.*, vol. 38, pp. 1433–1437, 1990.
[9] K. Kawano, K. Noguchi, T. Kitoh, and H. Miyazawa, "A finite element method (FEM) analysis of a shielded velocity-matched Ti:$LiNbO_3$ optical modulator," *IEEE Photon. Technol. Lett.*, vol. 3, pp. 919–921, 1991.
[10] T. Honma, and I. Fukai, "An analysis for the equivalence of boxed and shielded strip lines by a boundary element method," (Trans.: *IECE Japan*), vol. J65-B, pp. 497–498, 1982.
[11] T. Chang, and C. Tan, "Analysis of a shielded microstrip line with finite metallization thickness by the boundary element method," *IEEE Trans. Microwave Theory Tech.*, vol. 38, pp. 1130–1132, 1990.
[12] F. J. Schmückle and R. Pregla, "The method of lines for the analysis of planar waveguides with finite metallization thickness," *IEEE Trans. Microwave Theory Tech.*, vol. 39, pp. 107–111, 1991.
[13] S. A. Ivanov and G. L. Djankov, "Determination of the characteristic impedance by a step current density approximation," *IEEE Trans. Microwave Theory Tech.*, vol. MTT-32, pp. 450–452, 1984.
[14] S. Kosslowski, F. Bögelsack, and I. Wolff, "The application of the point-matching method to the analysis of microstrip lines with finite metallization thickness," *IEEE Trans. Microwave Theory Tech.*, vol. 36, pp. 1265–1271, 1988.
[15] C. Nguyen, "Broadside-coupled coplanar waveguides and their end-coupled band-pass filter applications," *IEEE Trans. Microwave Theory Tech.*, vol. 40, pp. 2181–2189, 1992.
[16] E. Drake, F. Medina, and M. Horno, "Quasi-TEM analysis of thick multistrip lines using an efficient iterative method," *Microwave Opt. Technol. Lett.*, vol. 5, pp. 530–534, 1992.

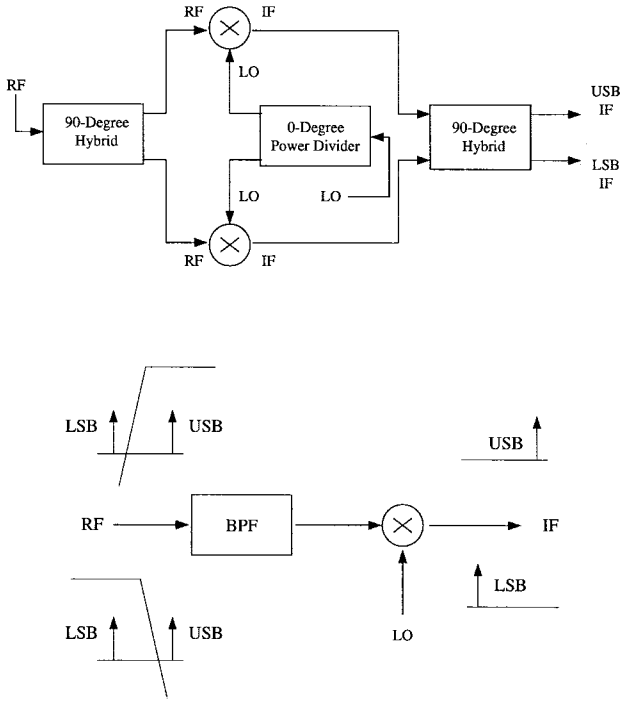

Fig. 1. Two different topologies in the design of SSB's (image rejection mixers).

Design of Lange-Couplers and Single-Sideband Mixers Using Micromachining Techniques

Chen-Yu Chi and Gabriel M. Rebeiz

***Abstract*—This paper reports on the design and performance of micromachined Lange-couplers and single-sideband mixers (SSB) on thin dielectric membranes at *Ku*-band. The micromachined Lange-coupler results in a 3.6±0.8 dB coupling bandwidth from 6.5 to 20 GHz. The Lange-coupler and an interdigital filter are used in a 17-GHz SSB. The SSB mixer requires 1–2 mW of local oscillator (LO) power without dc bias and achieves a 30 dB upper-sideband (USB) image rejection for an IF frequency of 1 GHz and above. The micromachined membrane technology can be easily scaled to millimeter-wave monolithic microwave integrated circuits (MMIC's) to meet the low-cost requirements in automotive or portable communication systems.**

***Index Terms*—Micromachining, single-sideband mixers.**

I. Introduction

Silicon micromachined technology has been used to build low-loss lumped elements, filters, and Wilkinson power dividers [1]–[3]. Recent research on micromachined stripline resonators and filters has demonstrated a conductor-loss limited performance at *K*- and *Ka*-band [4]. The micromachined components, suspended on thin dielectric membranes, do not suffer from dielectric loss and dispersion and can be used in the design of high-quality low-loss circuits at millimeter-wave frequencies. The purpose of this paper is to demonstrate the capability of micromachining technology to the design of integrated circuit modules. A single-sideband (SSB) mixer (also called an image-rejection mixer) is built and tested at *Ku*-band frequencies with applications in satellite communication systems and future millimeter-wave radiometers and automotive systems.

There are two different topologies in the design of single-sideband mixers (Fig. 1). The first topology is to use hybrid circuits to provide the required amplitude balance and phase shift to achieve the image rejection mixing. The advantage of this method is that a good isolation between the local ocsillator (LO), RF, and IF ports can be achieved and a low IF (0.01–2 GHz) can be extracted. However, the disadvantage of this design is that the performance of the SSB mixer strongly depends on the amplitude and phase balance of the hybrid circuits used and since this is difficult to achieve at millimeter-wave frequencies, this method is therefore seldom used in this frequency range. The second SSB mixer topology is to place a filter in front of a balanced mixer. The filter is designed to pass the RF frequency and reject the image frequency. This design employs only one balanced mixer and does not use an RF hybrid, LO power divider and IF-hybrid, resulting in a much smaller unit. A SSB mixer employing micromachining technology based on the second topology is presented here. The SSB mixer can be easily scaled to *V*-band (60 GHz) and *W*-band (77 GHz, 94 GHz) frequencies.

II. Design of the Micromachined Lange-Coupler

The analysis of a Lange-coupler is very similar to the analysis of interdigital filters and starts from the even- and odd-mode analysis of a pair of coupled-lines as described by [5]. In [5]'s analysis, the mutual coupling from nonadjacent lines is assumed to be small and

Manuscript received July 31, 1995; revised October 18, 1996. This work was supported by the National Science Foundation under the Presidential Young Investigator Award.

The authors are with the Electrical Engineering and Computer Science Department, University of Michigan, Ann Arbor, MI 48109-2122 USA.

Publisher Item Identifier S 0018-9480(97)00839-9.